ARTICLE NO. 79-4143

Satellite Drag Coefficients Calculated from Measured Distributions of Reflected Helium Atoms

Shih-Min Liu,* Pramod K. Sharma,† and Eldon L. Knuth‡
University of California, Los Angeles, Calif.

The primary objectives of this study were to obtain the necessary data and develop a calculation procedure that would facilitate predicting the atmospheric-helium contribution to the drag of a satellite having a predominantly convex exterior. Molecular-beam techniques were used to measure, for several incidence angles, the spatial and energy distributions of 7000 m/s helium atoms scattered from a 6061-T6 aluminum plate and an anodized 1235-0 aluminum surface. From these measured distributions, tangential and normal momentum accommodation coefficients were calculated as functions of incidence angle. Using these calculated accommodation coefficients, one can predict drag coefficients for satellites having predominantly convex exteriors. For spherical satellites, drag coefficients of 2.64 and 2.62 were predicted for the subject surfaces.

Introduction

VALUES of satellite drag coefficients are essential in such applications as extracting upper-atmosphere densities from the drag of aeronomy satellites and estimating satellite lifetimes for given atmospheric models. These drag coefficients can be obtained either directly from drag forces measured in the laboratory under conditions which simulate the satellite conditions or indirectly by calculating drag coefficients using, for each element of the satellite surface, measured values of the tangential and normal momentum-accommodation coefficients corresponding to the local incidence angle. For satellites circling the Earth at altitudes within the upper atmosphere, the contribution to the drag coefficient by He impinging at 7000 m/s (1.0 eV) is of particular interest.

Several studies of interactions of He with technical surfaces (e.g., polycystalline metal surfaces covered with adsorbed contaminants) do exist. (However, as will be noted, all of these studies were conducted with incident-atom energies an order of magnitude less than of interest here.) Several investigators obtained accommodation and drag coefficients. Thomas and Lord[1] measured the drag due to room-temperature He gas interacting with room temperature rotating steel spheres which had been baked at 450°C, and deduced tangential momentum coefficients of 0.824 and 1.040, respectively, for polished and roughened surfaces. They interpreted the value in excess of unity as indicative of backscattering (scattering back in the direction of the incident atoms). Lord[2] measured the drag due to room-temperature He gas interacting with room-temperature rotating disks (Mo, W, Ta, Pt, and Ti) which had been cleaned by rf induction heating. Recontamination of the surfaces was reduced by the use of chemical getters. Deduced tangential momentum accommodation coefficients ranged from 0.20 for Mo to 0.46 for Ta. Seidl and Steinheil[3] used a microbalance to measure the forces due to a room-temperature He beam (0.06 eV) impinging on several room-temperature surfaces, including a Cu surface with 5 μm grooves covered with adsorbed layers consisting chiefly of hydrocarbons and water. For this Cu surface, values of the tangential accommodation coefficient ranged from 1.16 at an incidence angle of 10 deg (relative to the surface normal) to approximately unity at incidence angles from 30 to 70 deg. The values greater than unity are considered to imply backscattering. Legge[4] measured drag coefficients for copper cones at surfaces temperatures up to 500°C and at He energies of 0.06 and 0.10 eV. For his conditions closest to those of interest here (He energy = 0.10 eV, surface temperature = 0.5 He stagnation temperature, and cone half angle = 45 deg), the value of the drag coefficient was 2.9 and was decreasing slowly with decreasing ratio of surface temperature to He stagnation temperature.

O'Keefe and Palmer[5] scattered a room-temperature (0.05 eV) He beam from room-temperature polished glass and shot-blasted glass surfaces and measured the scattering distributions in the plane of the incident beam and the surface normal. They observed more backscattering from the shot-blasted surface than from the polished surface and greater deviations from the cosine-scattering model at larger incidence angles (measured from the surface normal).

Note that the highest He energy realized in these several studies was 0.10 eV—an order of magnitude less than that of the He atoms at satellite speeds. This lack was due largely to the difficulty of generating freejets and/or molecular beams with these speeds. Note also the lack of normal momentum accommodation coefficients—even at low He energies.

Ab initio calculations of scattering from rough surfaces are relatively difficult—due partly to the difficulty of modeling the surface roughness. One of the most rewarding models (for the effort required) is, perhaps, that of Shawyer and Peggs.[6] They performed Monte Carlo calculations for atoms striking regularly spaced triangular grooves oriented transverse to the plane defined by the incident beam and the surface normal. Scattering from all surfaces was taken to be diffuse. For the geometries used, significant backscattering was calculated.

In the absence of more detailed information, drag is modeled frequently using normal-momentum and tangential-momentum accommodation coefficients; calculations are relatively convenient for the case in which these accommodation coefficients are independent of incidence angle. (Compare, for example, Ref. 7, Secs. V.7 and V.8.) For technical surfaces (e.g., polycrystalline metal surfaces with adsorbed contaminants), the accommodations are considered

Received Dec. 12, 1978; revision received April 24, 1979.

Index category: Rarefied Flows.

*Postdoctoral Scholar, Chemical, Nuclear, and Thermal Engineering Dept.; presently, California Computer Products, Inc., Anaheim Calif.

†Postdoctoral Scholar, Chemical, Nuclear, and Thermal Engineering Dept.; presently, MIT Energy Laboratory, Cambridge, Mass.

‡Professor of Engineering and Applied Science, Chemical, Nuclear, and Thermal Engineering Dept. Associate Fellow AIAA.

frequently to be complete; the molecules are considered to scatter with a cosine distribution and with an energy distribution characterized by the surface temperature. However, deviations from this model could alter the value of the drag significantly.

Hence, specific objectives of the present study included 1) measurements of scattering distribution as a function of incidence angle, 2) measurements of energy accommodation as a function of incidence angle and scattering direction, 3) evaluation of differential and overall momentum accommodation coefficients, and 4) calculation of the drag coefficient from the aforementioned results.

Measurements

A. Experimental Apparatus and Procedures

A schematic diagram of the molecular beam system used in the present study is shown in Fig. 1. The system has been described in detail by Hays et al.[8] and Liu.[9] The satellite speed (7000 m/s) helium beams were generated using the arc-heated supersonic-beam source developed by Young.[10] The incident beam was collimated by a 0.25-cm diam orifice placed between the collimation chamber and the detection chamber. The beam was characterized by a multidisk velocity selector similar to that described by Trujillo et al.[11]

The detection system was designed for facilitating measurements of the complete three-dimensional density and mean-energy distributions of satellite-speed helium atoms reflected from the aluminum surfaces. The system included a target-positioning mechanism, a detector-rotating mechanism, and a quadrupole mass spectrometer and/or a retarding-field energy analyzer. Descriptions of the first two mechanisms are given in Ref. 12. Readers interested in details of quadrupole mass spectrometers are referred to Ref. 13. A schematic diagram of the retarding-field energy analyzer (developed by Liu for use in these studies) is shown in Fig. 2 and described later in this section.

Spatial Distribution Measurements

Spatial distributions of the reflected helium beams were obtained by measuring the beam density with a laboratory-built quadrupole mass spectrometer. The mass spectrometer could be rotated in both the plane of the incident beam and the surface normal (-90 deg $< \theta_r < +90$ deg), and a perpendicular plane ($0 \leq \phi < 90$ deg); see Fig. 3. The angle of incidence varied from 0 to 90 deg by rotating the test surface. The mass spectrometer signal, proportional to the helium number density, was recorded on a chart recorder.

Energy-Distribution Measurements

The energy distributions were measured using the retarding-field energy analyzer shown in Fig. 2. An electron-impact ionizer, mounted 1.3 cm from the target surface on the entrance plate of the analyzer, ionizes a fraction of the beam species (also of the residual background). The retarding-field section of the analyzer consists of seven stainless-steel washer-shaped disks placed in a stainless-steel can. The inlet plate is followed by three focusing plates, a retarding plate, and two more focusing plates. Typical plate potentials also are given in Fig. 2. The ions that pass through the retarding-field region are filtered by a 5.1-cm quadrupole mass filter to eliminate the noise from the ionized background gases. The filtered ions are then detected by a pulse-counting particle detector. The energy spectrum of the reflected atoms at a given scattering position is obtained by measuring the reflected-beam density as a function of the retarding potential. The measured spectrum was processed by a NS 513 signal averager and recorded on IBM cards. For an earlier description, and some additional details, of this energy analyzer, see Ref. 14.

Although the electron-impact ionization does not change the kinetic energy of a helium atom (since the translational energy transfer between the ionizing electron and the atom is negligible due to the large ratio of their masses), it was found that space-charge effects of ionizing electrons in the ionization region and/or surface-charge effects on the anode cage did introduce a systematic shift of the entire energy spectrum toward lower energies (i.e., the positive ions were produced in a region of negative potential with respect to ground). To reduce this shift, a small emission current (~ 50 μA) was used in the ionizer. Also, a positive potential (8 V relative to ground) was applied to the anode cage in order to countershift the energy spectrum toward higher energies. Then, since the potential of the ionization region was no longer at ground level, it was necessary to ascertain independently a reference point in the energy spectrum. This reference point was provided by the thermal energy spectrum

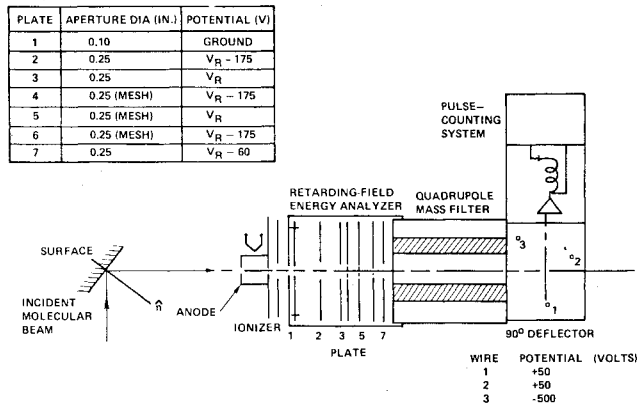

Fig. 2 Schematic diagram of the retarding field energy analyzer.

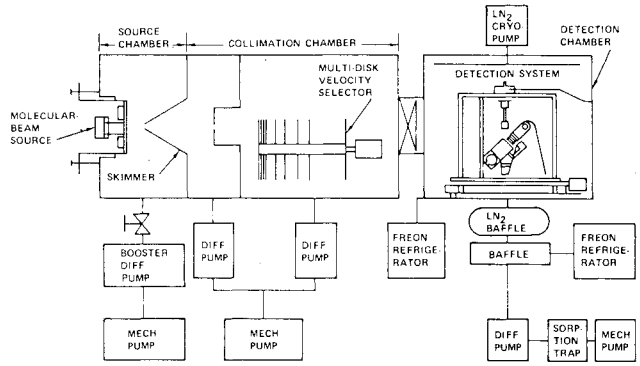

Fig. 1 Schematic diagram of the molecular beam system.

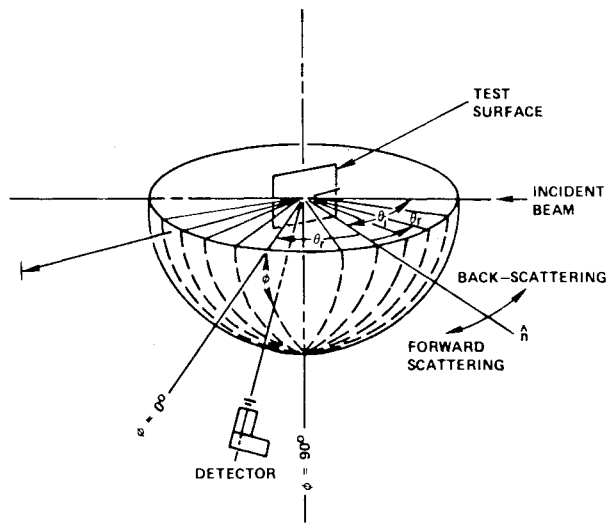

Fig. 3 Schematic diagram of the scattering system.

of the background gas, which has a mean thermal energy of 0.05 eV (i.e., the mean thermal energy at 296 K).

Since the background gas also contributed to the measured energy spectrum, it was necessary to subtract this contribution in order to obtain the reflected-beam energy distributions. For the (earlier) measurements on a 6061-T-6 surface, this subtraction was facilitated by measuring two spectra (one for the reflected beam plus background and one for the background alone) under the same operating conditions. Both the background spectrum and the reflected-beam spectrum were least-squares fitted using a high-order Chebyshev polynomial function. For the (later) measurements on an anodized 1235-0 surface, this subtraction was handled automatically by modulating the incident beam and feeding the reflected-beam signal to a lock-in amplifier.

The differential energy distributions $f(E)$, where $f(E)\,dE$ is proportional to the fraction of atoms with energy between E and $E+dE$, were obtained by simple differentiation of the fitted functions. Figure 4 shows typical normalized energy spectra of the thermal background and the reflected helium atoms (triangles and circles), their least-square fitted curves (dashed and solid curves), and the corresponding differential energy distributions. The mean reflected-beam energy at a given scattering position (cf. Fig. 3) was evaluated from

$$E_r(\theta_i,\theta_r,\phi) = \tilde{E}_r - \tilde{E}_{\text{ref}} + 0.05\ (\text{eV}) \tag{1}$$

where

$$\tilde{E}(\theta_i,\theta_r,\phi) = \int f(E)\cdot E\cdot dE \Big/ \int f(E)\,dE \tag{2}$$

and 0.05 eV is the thermal energy of the background gas at 296 K. The differential energy accommodation coefficient at a given scattering position was obtained using

$$\alpha_E(\theta_i,\theta_r,\phi) = [E_i - E_r(\theta_i,\theta_r,\phi)]/E_i \tag{3}$$

where E_i is the incident-beam energy. Note that in Eq. (3), the energy of atoms reflected at the surface temperature have been neglected (in the denominator) in comparison with the incident-beam energy E_i.

The energies E_i and E_r were approximated by $\frac{1}{2}mv_i^2$ and $\frac{1}{2}mv_r^2$, respectively, in order to obtain the reflected-beam velocity v_r from known values of α_E and v_i. These approximations are justified since helium is a monatomic gas and the incident and reflected beams have very narrow velocity distributions.

Surface Conditions

The surfaces (6061-T Al and anodized 1235-0 Al) were provided by personnel at the NASA Langley Research Center.

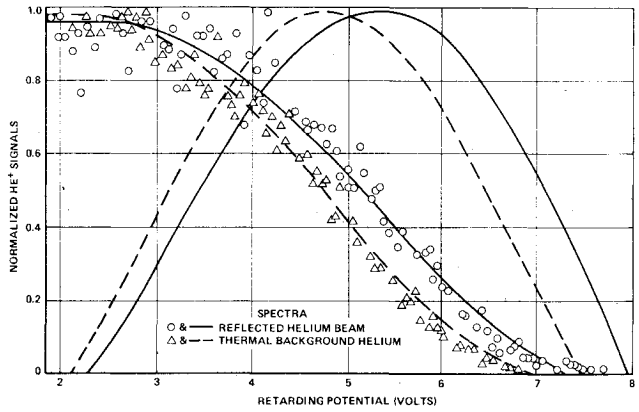

Fig. 4 Least-square fitted energy spectra of the reflected helium atoms and the thermal background helium gas.

They were cleaned with acetone prior to reducing the pressure in the detection chamber; no special in situ outgassing or conditioning was provided. All tests were conducted with the surfaces at room temperature; background pressures were typically of the order of 2×10^{-8} Torr. Possible contamination of the test surface by metals eroded from the arc-heater electrodes was concluded to be negligible on the basis of a comparison of the electrode-erosion rate with the arc-heater gas-flow rate. No changes of surface scattering with time (due to either addition or removal of surface contaminants) were noted.

B. Measured Values

Spatial Distributions

Both in-plane (i.e., in the plane containing the incident beam and the surface normal) and out-of-plane spatial distributions of reflected helium atoms were measured for six different incidence angles (0, 15, 30, 45, 60, and 75 deg from the surface normal). A typical spatial scattering distribution for a 6061-T6 Al surface and an incidence angle of 75 deg is shown in Fig. 5. The center of the polar diagram corresponds to the point of impingement. The incident beam impinges on the test surface (which coincides with the surface of the page) from the bottom of the diagram with the given incidence angle measured from the surface normal. The dashed lines at constant values of θ_r indicate detector paths (i.e., from $\phi=0$ deg to $\phi=90$ deg). Tabulated measurements for the anodized Al surface for an incidence angle of 15 deg are shown in Table 1. Similar scattering patterns were obtained for other incidence angles. The most interesting feature of these scattering patterns is the backscattering, particularly as the incidence angle increases toward the surface tangent (i.e., for large values of θ_i). This feature is qualitatively consistent with

Table 1 Differential energy accommodation coefficients and reflected-beam densities for 7000 m/s helium beam scattered from anodized aluminum surface at 15 deg incidence angle

ϕ, deg \ θ_r, deg	−75	−60	−45	−30	−15	0	15	30	45	60	75
0		65[a]						43	51	47	
		2.6[b]						4.2	3.5	2.35	
15		58						30	42	44	
		2.5						4.0	3.4	2.3	
30		62	53				44	49	43	38	
		2.3	3.1				4.2	3.75	3.2	2.1	
45		53	52	54	59	48	40	51	34		
		1.8	2.5	3.2	3.6	3.7	3.1	3.25	2.6		
60		47	46	48	45	43	34	28	25		
		1.5	2.0	2.3	2.6	2.7	2.7	2.3	2.0		
75											

[a] Differential energy accommodation coefficient (%). [b] Reflected-beam density (arbitrary units).

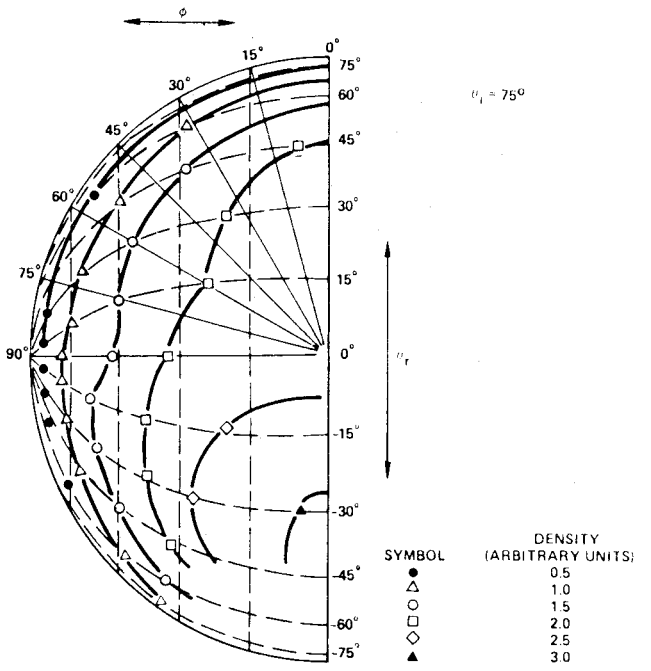

Fig. 5 Polar plot of scattered-beam density distribution for 7000 m/s helium beam scattered from cleaned 6061-T6 aluminum plate at 75 deg incidence angle.

the observations of Thomas and Lord,[1] Seidl and Steinheil,[3] and O'Keefe and Palmer.[5]

Additional polar plots of spatial scattering distributions for the 6061-T6 Al surface, an anodized Al foil, a white paint surface, and a quartz surface are given in Ref. 12. Tabulated measurements for the 6061-T6 Al surface are given in Refs. 14 and 15. Both polar plots and tabulated measurements for the anodized Al surface are given in Ref. 15.

Energy Accommodation Coefficients

Differential energy accommodation coefficients were obtained from measured energy distributions by use of Eqs. (1-3). Energy distributions were measured for six different incidence angles ($\theta_i = 0$, 15, 30, 45, 60, and 75 deg from the surface normal). For each incidence angle, distributions were measured at approximately forty scattering positions. These scattering positions were chosen from eleven in-plane scattering angles ($\theta_r = \pm 75$, ± 60, ± 45, ± 30, ± 15, and 0 deg, and six out-of-plane scattering angles ($\phi = 0$, 15, 30, 45, 60, and 75 deg). Measurements were not possible within a solid angle around the incident beam (due to interference between the detector and the incident beam at these scattering positions) and for some glancing scattering angles (due to weak signal-to-noise ratios).

Typical values of the differential energy accommodation coefficients obtained for an anodized 1235-0 Al surface at 15 deg incidence angle also are shown in Table 1. Additional values for this surface are given in Ref. 15. Values for the 6061-T6Al surface are given in Refs. 14 and 15.

Momentum Accommodation Coefficients

Differential momentum accommodation coefficients may be defined as

$$\alpha_{NM} = \frac{(p_i - p_r)_N}{(p_i - p_w)_N} = \frac{(v_i - v_r)_N}{(v_i - v_w)_N} \tag{4}$$

$$\alpha_{TM} = \frac{(p_i - p_r)_T}{p_{i_T}} = \frac{(v_i - v_r)_T}{v_{i_T}} \tag{5}$$

where α_{NM} and α_{TM} are normal and tangential differential momentum accommodation coefficients, respectively, subscript N refers to the normal component, and subscript T to the tangential component. The velocity components are given (compare Fig. 3) by

$$v_{i_N} = v_i \cos\theta_i \tag{6a}$$

$$v_{r_N} = v_r \cos\phi \cos\theta_r \tag{6b}$$

$$v_{i_T} = v_i \sin\theta_i \tag{6c}$$

$$v_{r_T} = -v_r \cos\phi \sin\theta_r \tag{6d}$$

Note that v_{i_N} and v_{r_N} are in opposite directions, whereas v_{i_T} and v_{r_T} are in the same direction. The component v_{w_N} is evaluated by averaging the normal component $u\cos\theta$ for a half-Maxwellian velocity distribution. One obtains

$$v_{w_N} = \sqrt{\frac{\pi}{2}\frac{kT}{m}} \tag{6e}$$

where k is Boltzmann constant and m is molecular mass. The direction of v_{w_N} also is opposite to that of v_{i_N}.

Overall Normal and Tangential Momentum Accommodation Coefficients

Overall normal and tangential momentum accommodation coefficients $\bar{\alpha}$ were calculated for each incidence angle by averaging over the differential coefficients α_i, taking into account the flux distribution and the solid angle represented by each measurement. Thus, the overall accommodation coefficient was deduced from the differential coefficients using

$$\bar{\alpha} = \sum_i j_i \alpha_i (\Delta\omega)_i \Big/ \sum_i j_i (\Delta\omega)_i$$

where j_i is the flux and $(\Delta\omega)_i$ the solid angle corresponding to the measurement. Since j_i is proportional to $n_i\sqrt{1-\alpha_{E_i}}$ and $(\Delta\omega)_i$ to $\cos\phi_i$, one may write

$$\bar{\alpha} = \sum_i n_i \sqrt{1-\alpha_{E_i}}\ \alpha_i \cos\phi_i \Big/ \sum_i n_i \sqrt{1-\alpha_{E_i}}\ \cos\phi_i \tag{7}$$

where n_i is the number density, α_{E_i} is the energy-accommodation coefficient, and ϕ_i is the out-of-plane scattering angle measured from the plane of incidence.

Evaluation of the Drag Coefficients

A drag coefficient was obtained from measured spatial and energy distributions for each of the two surfaces studied. The procedure followed is indicated in this section.

Recall that scattering and energy distributions could not be measured in a significant portion of the backscattering regions (due to interference of the detector with the beam) and additionally for large values of the scattering angle θ_r and the azimuthal angle ϕ (due to the weak signal-to-noise ratio). The following method was devised to extrapolate the measurements to these regions where measured values are not available.

If, for a given value of θ_i, one plots the scattering distributions measured in two orthogonal planes (one plane defined by a constant value of ϕ, the other by a constant value of θ_r), then the scattered-beam density at the intersection of these two planes must be common to both planes. Thus, the density at a particular point could be determined, if the values in its vicinity in two orthogonal planes passing through this point were known, by extrapolating in both planes to a common value of this point. The estimated value at this point could be used now in the estimation of the density at a new

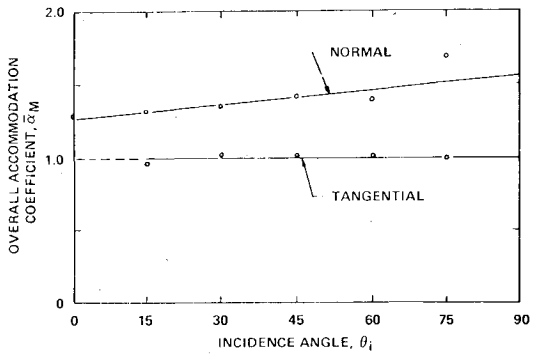

Fig. 6 Overall normal and tangential momentum accommodation coefficient as a function of incidence angle for cleaned 6051-T6 aluminum surface.

point in its vicinity. This procedure was used to fill in the gaps in Table 1, also for other incidence angles for both surfaces under study.

Differential normal and tangential momentum accommodation coefficients were determined by use of Eqs. (4-6). Overall normal and tangential momentum accommodation coefficients were then determined by Eq. (7) for each incidence angle. A plot of the overall normal and tangential momentum accommodation coefficients vs the incidence angle θ_i is shown in Fig. 6 for the 6061-T6 Al surface. A similar plot was obtained for the anodized Al surface.

Calculation of the Drag Coefficient from Measured Accommodation Coefficients

An expression for the drag coefficient for a sphere moving in a rarefied atmosphere was derived for the case in which the random (thermal) molecular speeds are negligible in comparison with the satellite speed. Expressing the force exerted on a toroidal differential area dA as a function of the average normal and tangential momentum accommodation coefficients (functions of θ_i), summing over the upper half of the sphere, and equating this total force to $\frac{1}{2}C_D\rho V_\infty^2 A$, one obtains

$$C_D = \frac{4}{V_\infty}\sum_{\theta_i=0}^{\pi/2}\left[(V_\infty - V_w)_N(\alpha_{NM}\cos\theta_i) + (V_\infty - V_w)_T(\alpha_{TM}\sin\theta_i)\right]\cdot\sin\theta_i\cos\theta_i\Delta\theta_i \qquad (8)$$

where α_{NM} and α_{TM} are, respectively, overall normal and tangential momentum accommodation coefficients (a function of θ_i), V_∞ is the incident speed of the beam for which the experimental measurements are made, and V_w is the average reflected speed for complete accommodation with the surface.

The drag coefficients for the two surfaces under study were computed from Eq. (8) by numerical integration using the results in Fig. 6 for the 6061-T6 Al surface and a similar plot for the anodized 1235-0 Al surface. For the 6061-T6 Al surface, $C_D = 2.64$ was found; for the anodized 1235-0 Al surface, $C_D = 2.62$.

Discussion

As indicated in Fig. 6, the overall tangential momentum accommodation coefficient was found to be approximately unity for the investigated range of incidence angles. This result implies that, for the investigated surfaces, the tangential momentum associated with the observed backscattering is approximately cancelled by the tangential momentum associated with the observed forward scattering. This value agrees within a few percentage points with the values obtained by Thomas and Lord[1] for much lower He energies and a roughened steel surface, also within a few percentage points with the values obtained by Seidl and Steinheil[3] for a 0.06 eV He beam, a grooved Cu surface, and $\theta_i \gtrsim 30$ deg, but about 15% less than obtained by Seidl and Steinheil for $\theta_i = 10$ deg.

The value of the drag coefficient obtained for both surfaces is about 2.6. This value is about 30% greater than the value calculated for either specular reflection with arbitrary surface temperature or diffuse reflection with the scattered-particle speed much smaller than the incident-particle speed. This high value of the drag coefficient arises due to the prominent backscattering of the incident helium atoms observed in the scattering patterns. This backscattering could be due to the gross surface roughness and/or the relative lattice softness of the aluminum satellite surfaces.

Recall that the expression for the drag coefficient [Eq. (8)] was derived for the case of large-speed ratios. The derivation of an expression that takes into account the random molecular speeds in the atmosphere is more difficult. However, for the particular case when the normal and tangential momentum accommodation coefficients are constant, a relatively simple expression for the drag coefficient may be derived in terms of the speed ratio $S(=V_\infty/\sqrt{2kT/m})$ [see e.g., Ref. 7, p. 167, Eq. (16)]. This predicted dependence on S, and some experimental points obtained for He, are shown in Fig. 38 of Ref. 7. These results establish that for S greater than about 2.4, the drag coefficient approaches a terminal value and becomes relatively independent of the speed ratio. Thus, the expression for the drag coefficient given here is sufficiently accurate for many satellite conditions.

Acknowledgments

This research was supported by NASA under Grant No. NGR 05-007-416. The assistance of W. E. Rodgers, Principal Electronics Technician, in the construction of the equipment used here is greatly appreciated.

References

[1] Thomas, L. B. and Lord, R. G., "Comparative Measurements of Tangential Momentum and Thermal Accommodations on Polished and on Roughened Steel Spheres," *Rarefied Gas Dynamics*, edited by K. Karamcheti, Academic Press, New York, 1974, pp. 405-412.

[2] Lord, R. G., "Tangential Momentum Accommodation Coefficients of Rare Gases on Polycrystalline Metal Surfaces," AIAA *Progress in Astronautics and Aeronautics, Rarefied Gas Dynamics*, Vol. 51, Pt. I, edited by J. L. Potter, New York, 1977, pp. 531-538.

[3] Seidl, M. and Steinheil, E., "Measurement of Momentum Accommodation Coefficients on Surfaces Characterized by Auger Spectroscopy, SIMS, and LEED," *Rarefied Gas Dynamics*, edited by M. Becker and M. Fiebig, paper E 9, DFVLR-Press, Porz-Wahn, W. Germany, 1974.

[4] Legge, H., "Drag and Heat Transfer Measurements of Cones at Different Wall Tempertures in Free and Near Molecule Flow," *3. Symposium Gas-Oberflächen-Wechselwirkung vom 6.-8.Okt.1975, Teil 1: Gasreibung und aerothermische Erhitzung im Bereich der Strömung verdünnten Gase*, K.-H. Gronau and H. Rieger, eds., DOKZENTBw, Bonn, W. Germany, 1977, pp. 47-60.

[5] O'Keefe, D. R. and Palmer, R. L., "Atomic and Molecular Beam Scattering from Macroscopically Rough Surfaces," *Journal of Vacuum Science and Technology*, Vol. 8, Jan./Feb. 1971, pp. 27-30.

[6] Peggs, G. N., "The Scattering of Molecules from a Rough Surface," National Physical Laboratory, Teddington, England, NPL Rept. MOM 21, June 1976.

[7] Patterson, G. N., *Introduction to the Kinetic Theory of Gas Flows*, University of Toronto Press, Toronto, 1971.

[8] Hays, W. J., Rodgers, W. E., and Knuth, E. L., "Scattering of Argon Beams with Incident Energies up to 20 eV from a (111) Silver Surface," *Journal of Chemical Physics*, Vol. 56, Feb. 1972, pp. 1652-1657.

[9] Liu, S.-M., "An Experimental Study of Interactions of Hyperthermal Atomic Beams with (111) Silver Surfaces and Adsorbed Molecules," UCLA School of Engineering and Applied Science, Los Angeles, Calif., UCLA-ENG-7510, Feb. 1975.

[10]Young, W.-S., Rodgers, W. E., and Knuth, E. L., "An Arc Heater for Supersonic Molecular Beams," *Review of Scientific Instruments*, Vol. 40, Oct. 1969, pp. 1346-1347.

[11]Trujillo, S. M., Rol, P. K., and Rothe, E. W., "Slotted-Disk Velocity Selector of Extended Range," *Review of Scientific Instruments*, Vol. 33, Aug. 1962, pp. 841-843.

[12]Liu, S.-M. Rodgers, W. E., and Knuth, E. L., "Interactions of Satellite-Speed Helium Atoms with Satellite Surfaces. I: Spatial Distributions of Reflected Helium Atoms," UCLA School of Engineering and Applied Science, Los Angeles, Calif., UCLA-ENG-7546, June 1975.

[13]*Quadrupole Mass Spectrometry and Its Applications*, Dawson, P. H., ed., Elsevier Scientific Publishing Co., New York, 1976.

[14]Liu, S.-M. and Knuth, E. L., "Interactions of Satellite-Speed Helium Atoms with Satellite Surfaces. II: Energy Distributions of Reflected Helium Atoms," UCLA School of Engineering and Applied Science, Los Angeles, Calif., UCLA-ENG-7638, April 1976.

[15]Sharma, P. K. and Knuth, E. L., "Interactions of Satellite-Speed Helium Atoms with Satellite Surfaces. III: Drag Coefficients from Spatial and Energy Distributions of Reflected Helium Atoms," UCLA School of Engineering and Applied Science, Los Angeles, Calif., UCLA-ENG-7857, Sept. 1978.